Solution Structure and Dynamics of Cartilage Aggrecan

A. Papagiannopoulos,[†] T. A.Waigh,*[,†] T. Hardingham,[‡] and M. Heinrich[§]

Biological Physics, Department of Physics and Astronomy, University of Manchester, PO Box 88, Manchester, M60 1QD United Kingdom, Faculty of Life Sciences, Michael Smith Building, University of Manchester, Oxford Road, Manchester, M13 9PT United Kingdom, and Institut für Festkörperforschung, Forschungszentrum Jülich, D-52425 Jülich, Germany

Received March 24, 2006; Revised Manuscript Received May 3, 2006

We studied the structure and dynamics of porcine laryngeal aggrecan in solution using a range of noninvasive techniques: dynamic light scattering (DLS), small-angle neutron scattering (SANS), video particle tracking (VPT) microrheology, and diffusing wave spectroscopy (DWS). The data are analyzed within the framework of a combined static and dynamic scaling model, and evidence is found for reptation of the comb backbones with unentangled side-chain dynamics. Small-angle neutron scattering indicated standard polyelectrolyte scaling of the mesh size (ξ) with concentration (c) in semidilute solutions for the whole aggrecan aggregate, $\xi = Ac^{-0.47\pm0.04}$, with the prefactor (A) implying there is on average 60 nm between the aggrecan subunits along the backbone. VPT demonstrated large exponents for the power law dependence of the intrinsic viscosity (η) on the polymer concentration in the semidilute concentration regime, $\eta \sim c^{\alpha}$; with α equal to 2.04 ± 0.06 and 1.95 ± 0.08 for the assembled and disassembled aggrecan aggregates, respectively. DWS at high frequencies (10^4-10^5 Hz) gave evidence for internal Rouse modes of the aggrecan monomers, independent of the degree of self-assembly of the molecules.

Introduction

The structure and dynamics of comb polyelectrolytes still provides many open questions.[1−6] The biological comb polyelectrolyte systems, the proteoglycans (long carbohydrate polymers attached to a protein) and glycoproteins (short carbohydrate polymers attached to a protein), remain some of the least well understood biopolymer systems in molecular biology.[7,8] This is caused by a series of complicating factors including chemical heterogeneity, noncrystallinity, and long-range charge interactions. Similarly, the synthetic biomimetic counterparts of proteoglycans and glycoproteins have only slowly begun to attract serious research interest.[2,9] Previously, we examined model polystyrene sulfonate (PSS) comb polyelectrolytes and established some simple relationships between their structure and viscoelasticity.[1,2] Due to the flexibility of the side-chains, the PSS combs would be considered a biomimetic proteoglycan system.

In another previous study on a biological comb system, concentrated solutions of porcine stomach mucin glycoprotein solutions were examined. Evidence was found for liquid crystallinity[3,10] and entanglement coupling between the comb molecules in concentrated solutions. A rich variety of phase behavior is thus possible in comb polyelectrolyte solutions.

Practically, we are motivated in the research on aggrecan (a proteoglycan bottle brush of bottle brushes, Figure 1) by biomedical questions relating to its function in diseased tissues. For example, the loss of the charge fraction in aggrecan molecules is strongly implicated in osteoarthritis conditions[11]

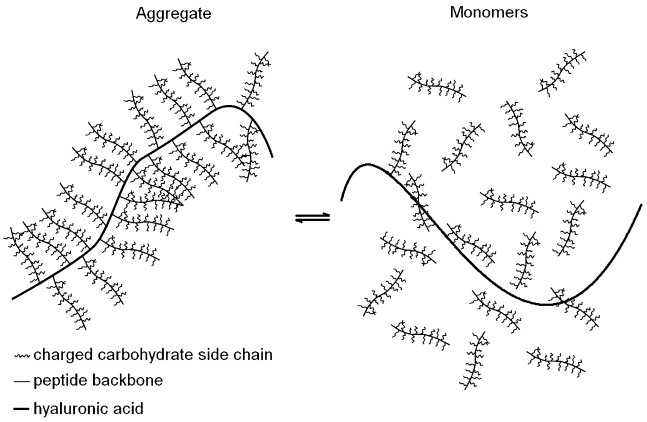

Figure 1. Schematic diagram of the process of self-assembly of aggrecan aggregate from monomer and hyaluronic acid.

and the highly viscous behavior of aggrecan is vitally important in its action as the compliant matrix between collagen fibers in many soft composite tissues.[12,13] Aggrecan provides the dominant mechanism of energy dissipation in a range of naturally occurring shock absorbing tissues.

In the literature, there is only a small amount of information on the solution state rheology of both side-chain liquid-crystalline and comb polymers. This contrasts with the situation of the melt dynamics of comb[14] and side-chain liquid-crystalline polymers,[15,16] which have experienced a number of studies. Recent experiments by our group examined the linear viscoelasticity of polyelectrolyte (polystyrene sulfonate) combs over a wide range of frequencies ($0.01-10^6$Hz).[2] At low frequencies the materials were predominantly viscous and the comb architecture had a dramatic effect on the magnitude and scaling of the viscosity with polymer concentration. In contrast, at high frequencies, diffusing wave spectroscopy demonstrated no effect of the comb architecture on the Rouse modes in the sample. A dynamic scaling model was derived for the unentangled

* To whom correspondence should be addressed. E-mail: t.a.waigh@manchester.ac.uk.

[†] Biological Physics, Department of Physics and Astronomy, University of Manchester.

[‡] Faculty of Life Sciences, Michael Smith Building, University of Manchester.

[§] Institut für Festkörperforschung.

10.1021/bm060287d CCC: $33.50
Published on Web 06/10/2006

semidilute viscoelasticity of sparsely branched combs and was in good agreement with both microrheology and small-angle X-ray scattering data.[1,2] The SAXS results of comb polyelectrolytes indicate that the semidilute correlation length is independent of comb architecture, providing a sound structural model with which to develop a theory of comb dynamics. In the dynamic scaling model for combs, the relaxation time of the backbone was renormalized by an average of the Rouse time of the attached side-chains, providing an additional polymer concentration dependence (an additional $c^{1/2}$ dependence, where c is the polymer concentration) for the viscosity (low-frequency dynamics) of the comb solutions compared with that for a linear flexible polyelectrolyte.[2] The high-frequency viscoelasticity of the PSS combs was in reasonable agreement with a scaling model for the dynamics of linear flexible polyelectrolytes.

Previous rheological studies on aggrecan aggregates have found that solutions demonstrated shear thinning behavior and the attachment of pendant comb side units caused an increase in the modulus of the material linearly proportional to the number of attached side-chains.[17−19] The aggrecan polymers are unassociating and do not form gels. To date no models have been developed that connect the molecular structure of the aggrecan aggregates to their rheological properties. The rheological properties of aggrecan are vitally important to model the viscoelasticity of cartilage and the action of boundary lubricants in synovial joints.[20,21] Furthermore, we believe the comparison of the physical behavior of aggrecan to synthetic comb polyelectrolytes will allow the development of effective synthetic treatments for osteoarthritis.[2]

Hyaluronic acid (the backbone of aggrecan) has been shown to act like a flexible hydrophilic polyelectrolyte in light scattering, small-angle X-ray scattering[22] (with a persistence length in dilute solutions of 6 nm), and rheology studies.[23,24] In semidilute solutions with SAXS,[25] the extension ratio (B = contour length/end to end length) is found to be 1.39 (a fairly extended conformation) for sodium hyaluronate compared to 3 for polystyrene sulfonate (a standard flexible polyelectrolyte). Atomic force microscopy images of whole aggrecan aggregate molecules indicate a large increase in the persistence length of the hyaluronic backbone when aggrecan monomers are attached and it becomes on the order of ∼100 nm.[26]

The structure and dynamics of flexible polyelectrolytes have recently experienced a number of important advances.[23,27,28] Dynamic scaling theories provide a simple robust motivation for both the morphology and viscoelasticity of flexible polyelectrolyte solutions, which have a number of novel features compared with their neutral counterparts, e.g., the relaxation time of linear flexible polyelectrolytes in entangled semidilute solutions is concentration independent.

Previous small-angle neutron scattering (SANS) studies have examined the structure of dilute aggrecan subunits,[29] but have not been extended into the semidilute regime. Aggrecan molecules typically function in the semidilute regime (∼5%w/w) in cartilage, so semidilute studies would directly relate to the molecules' biological function. In the current article, we study the structure of concentrated solutions of aggrecan for the first time with SANS.

A range of microrheology techniques have recently been developed to study the viscoelasticity of complex fluids, and these demonstrate good agreement with bulk rheology measurements in the case of flexible polyelectrolyte samples.[30] Microrheology presents a series of advantages over traditional rheological techniques; the measurements are noninvasive and will not damage delicate biological molecules, they require minute (∼20 μL) amounts of sample, they extend the measurable range of frequencies by 3 orders of magnitude, and they can be used to quantify the heterogeneities in solutions.[31] Aggrecan has not been previously examined with microrheology techniques, but the sizable viscosity of the solutions at low polymer concentrations makes it ideal for both particle tracking and diffusing wave spectroscopy measurements.[30] Therefore, we were able to measure the viscoelasticity of aggrecan at ultrafast frequencies (∼10^5Hz) for the first time and model the dynamics in terms of the screened hydrodynamic fluctuations (Rouse modes) of flexible polyelectrolyte chains.[28]

In the present article, we analyze the structure and dynamics of aggrecan using a novel range of noninvasive probes. The data are analyzed in the framework of scaling theories for flexible polyelectrolytes[2,27] and the connection is made to the physical behavior of synthetic polyelectrolyte combs. A dynamic scaling theory is derived to account for the reptation of flexible polyelectrolyte combs with both unentangled and entangled side-chains. We believe the new detailed picture of aggrecan viscoelasticity we present will be invaluable in the construction of new molecular models for the dissipative properties of cartilages[11] and the action of aggrecan in the reduction of friction in synovial joints.[20,21]

Materials and Methods

Aggrecan Samples. Aggrecan was provided both in the aggregated and the monomeric state (Figure 1). In the aggregated state, aggrecan monomers are physically bound onto a hyaluronic acid chain. Aggrecan monomers consist of a ∼400 nm protein backbone with approximately one hundred highly negatively charged side chains, each ∼40 nm in length which are predominantly chondroitin sulfate glycosaminoglycan (CS-GAG).[32,33] Additional shorter side-chains of keratan sulfate also occur. Aggrecan is found in cartilage, mainly as aggregates involving hyaluronic acid (major axis of the ellipsoid is ∼2000 nm).[32] The aggregate is thought to consist of an extended hyaluronic acid chain to which the aggrecan monomers are regularly attached. Each aggrecan monomer has a globular protein head which binds to the hyaluronic acid backbone.

Experiments on aggrecan could be performed in both the aggregated and the monomeric state. Aggrecan and its link-stable aggregate were prepared from porcine laryngeal cartilage.[34,35] Sliced fresh cartilage was extracted in 4 M guanidine HCl containing proteinase inhibitors, and the aggregates were reformed and purified by density gradient centrifugation in CsCl under associative conditions. Monomeric aggrecan was prepared from aggregates by a second CsCl density gradient centrifugation under dissociative conditions in the presence of 4 M guanidine HCl. The aggrecan samples were left to equilibrate for at least 48 h before any experiment.

Dynamic Light Scattering. Dynamic light scattering measurements were performed on an ALV 5000 goniometer using a fast multi τ digital correlator which provided correlation times in the range from 12.5 ns to 1000 s. The light source was a 5 W Spectra Physics argon ion laser 2016 Stabilite operating at 488 nm and 140 mW. The vv configuration was used with parallel polarizers before the sample cuvette and after the laser. Field autocorrelation functions were obtained at a series of angles in the range 30−120°. Samples were filtered with 0.45 μm Supor membrane filters into standard 1 cm diameter Helma quartz cells.

Small Angle Neutron Scattering. Small angle neutron scattering (SANS) experiments were performed on the KWS2 station at the research reactor FRJ2 (Forschungszentrum Julich GmbH), a classical pinhole instrument with a typical q range ($q = (4\pi/\lambda)\sin\theta/2$, λ is the wavelength of the neutrons and θ is the scattering angle) from about 10^{-3} to 0.2 Å^{-1} (real space 1000−10 Å). The wavelength of the neutrons was 7 Å, and the sample−detector distances used were 2, 8, and 20 m. Aggrecan was studied in semidilute solutions in D_2O and

each sample was allowed to equilibrate for over a day to provide complete exchange of all labile hydrogens.

Microrheology. The extraction of the rheological properties of complex fluids through the investigation of the motion of probe particles immersed into the fluid is a standard technique in microrheology.[30,36] The thermal motion of a spherical particle coupled with a polymer network is affected by the viscoelastic properties of the medium. The time evolution of the mean squared displacement (MSD) of the particle contains rheological information on the viscoelastic medium.[37] The time evolution of the MSD versus time plot in a log−log representation always has a slope between 0 (purely elastic) and 1 (purely viscous). The evolution of the slope with time reflects the different nature of response of a viscoelastic material at different time scales.

In the case of an incompressible medium and a particle with nonslip boundary conditions, a generalized Stokes−Einstein relation (GSER) can be used[37] in order to connect the MSD with the viscoelastic properties of the complex fluid

$$\tilde{G}(s) = \frac{k_B T}{\pi a s \langle \Delta \tilde{r}^2(s) \rangle} \quad (1)$$

where $\tilde{G}(s)$ is the shear modulus as a function of the Laplace frequency s and $\langle \Delta \tilde{r}^2(s) \rangle$ is the Laplace transform of the MSD. The Fourier transform of $G(t)$ is the complex shear modulus $\tilde{G}^*(\omega) = G'(\omega) + iG''(\omega)$, with ω the Fourier frequency. The storage (G') and loss (G'') moduli as a function of frequency can be calculated from the MSD as a function of time.

In video particle tracking microrheology, we simultaneously analyzed the trajectories of hundreds of particles and the viscoelastic moduli were extracted in the range of 0.1−25 rad/s (0.04−10 s temporal range). For diffusing wave spectroscopy a concentrated dispersion of probe particles was used to ensure the multiple scattering of light, and the viscoelastic moduli were extracted in the range of 10^4−10^7 rad/s (10^{-7}−10^{-4} s temporal range). With a combination of the two microrheology techniques it was possible to investigate the dynamics of aqueous aggrecan samples over a wide range of frequencies.

Particle Tracking Microrheology. Particle tracking microrheology was performed on monomeric and aggregated aggrecan in pH 7.4 EDTA buffer with 0.15 M NaCl. Amino-functionalized polystyrene particles of 0.495 μm diameter were used. The concentration of the particles was such that about 40−50 of them were tracked simultaneously. The thermal motion of the particles was measured with an Olympus OH2 microscope connected to a black and white Jaitisu CCD camera. A 100× oil immersion lens was used to focus into the sample well, approximately 15 μm underneath the cover slip. The trajectories of the probe particles were analyzed with a modified version of the IDL tracking software developed by Weeks et al.[38] in order to obtain the mean squared displacement (MSD) as a function of lag time.

Two-point probe correlation was also used to confirm the reliability of the one-point correlation[39] for the measurement of the bulk properties of the solutions. Where it is not explicitly mentioned, the MSD data we present were calculated using the one-point correlation method.

Diffusing Wave Spectroscopy. Experiments were performed on the ALV5000 light scattering instrument in transmission geometry[40] with crossed polarizers. The probe particles were identical to those used in particle tracking experiments, but at much higher concentrations (0.5% w/w) in order to ensure they were in the multiple scattering regime. Experiments were run for about 1 h for each sample so that low noise intensity autocorrelation functions were obtained. The transport mean free path (l^*) was calibrated by a dispersion of particles in pure water and the mean squared displacement data was inverted to provide the viscoelastic moduli.[41]

The field autocorrelation function $g_1(t)$ for the transmission geometry can be written as

$$g_1(t) = \int_0^\infty P(s) \exp\left(-\frac{1}{3} k_0^2 \langle r^2(t) \rangle s/l^*\right) ds \quad (2)$$

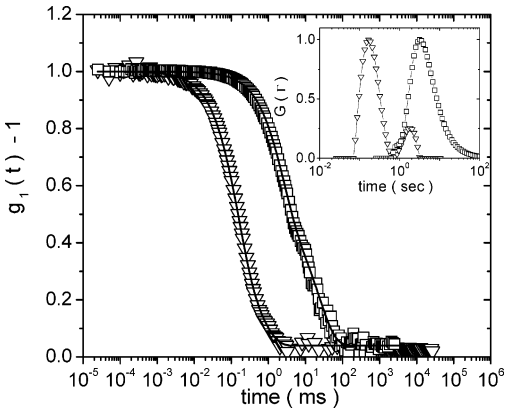

Figure 2. Normalized field auto-correlation functions collected at 30° (squares) and 120° (triangles) from aggrecan monomer at 0.5 mg/mL in 0.15 M NaCl in pH 7.4 EDTA buffer. The lines are fits with eq 3. Inset: Distribution functions for 30° (squares) and 120° (triangles) corresponding to the correlation functions.

where $P(s)$ is the path length distribution, $\langle r^2(t) \rangle$ is the mean square displacement, and k_0 ($=2\pi/\lambda$) is the wavevector (λ = 488 nm is the wavelength of light). The field autocorrelation function $g_1(t)$ is obtained from the measured intensity autocorrelation function $g_2(t)$ using the Siegert relationship $g_2(t) = 1 + \beta g_1^2(t)$, where β is a constant, which depends on the instrument and is equal to unity in an ideal experiment. The MSD can thus be extracted numerically from the measured field autocorrelation function by the use of the above integral relation for $g_1(t)$. More details about the experimental microrheology procedures can be found in a publication on synthetic polyelectrolyte combs.[2]

Results

Dynamic Light Scattering. Dynamic light scattering (DLS) was used to investigate aggrecan aggregate solutions in both assembled and disassembled states (Figure 1). The disassembled state was achieved by dissolving the aggregated material in a buffered solution of pH 4. Under these conditions the monomers are dissociated from the hyaluronan chain. There was no detectable difference in the DLS experiments, between samples created in the monomeric state by CsCl centrifugation and samples prepared by dissolving aggregated material at pH 4. The assembled aggrecan samples were prepared in pH 7.4 EDTA buffered solutions with 0.15 M NaCl. The auto-correlation functions collected using dynamic light scattering from aggrecan samples (aggregated and monomeric) showed either a broad distribution of relaxation rates or a bimodal distribution of relaxation rates (Figure 2), with a constant background offset corresponding to the long time motion of the aggregates. The distribution function at 120° is clearly bimodal. The case of 30° shows a broad distribution of relaxation times. The field auto-correlation functions ($g_1(t)$) were analyzed by fitting a double exponential with a constant offset (Figure 2)

$$g_1(t) = a_{\text{internal}} \exp(-\Gamma_{\text{internal}} t) + a_{\text{monomer}} \exp(-\Gamma_{\text{monomer}} t) + a_{\text{aggregate}} \quad (3)$$

where a_{internal}, a_{monomer}, and $a_{\text{aggregate}}$ are the amplitudes for the internal dynamic mode of the monomers, translational diffusion of the monomers and translational diffusion of the aggregates, respectively. Γ_{internal} and Γ_{monomer} are the relaxation rates of the internal mode and the translational diffusion of the monomer, respectively. This gives a robust representation of the data without making any assumptions about the polydispersities of

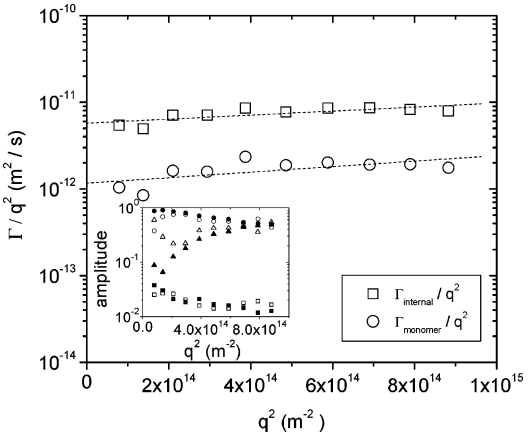

Figure 3. Apparent diffusion coefficient Γ/q^2 as a function of q^2 for aggrecan monomer at 0.5 mg/mL in 0.15 M NaCl in pH 7.4 EDTA buffer. The dashed lines are linear fits to the data. Circles indicate the translational diffusion of the monomer and squares indicate internal diffusive motion of the monomers. Inset: The amplitudes for the fit of eq 3 to the correlation functions are shown as a function of q^2. Filled symbols indicate the aggregated sample, open symbols the monomeric sample, triangles the internal mode, circles the monomer mode, and squares the aggregate mode.

the components, which are difficult to quantify with branched charged polymers (there are a large variety of electrostatic environments for the counterions).

The two distinct relaxation rates (Γ_{internal} and Γ_{monomer} with $\Gamma_{\text{internal}} > \Gamma_{\text{monomer}}$) correspond to two different dynamic modes in the sample. The intensity auto-correlation function ($g_2(t)$) is related to the field auto-correlation function ($g_1(t)$) using the Siegert relationship

$$g_2(t) = 1 + \beta g_1^2(t) \tag{4}$$

where β is the contrast factor.

The resulting apparent diffusion coefficients ($D_{\text{internal}} = \Gamma/q^2$) for the internal modes of the aggrecan monomer at 0.5 mg/mL in 0.15 M NaCl pH 7.4 EDTA buffer as a function of squared scattering vector (q^2) are shown in Figure 3. Both internal and monomer relaxation processes indicate diffusive behavior; that is, the apparent diffusion coefficient Γ/q^2 has little q dependence. Extrapolating the data of Figure 3 to zero q^2 using a linear fit, we calculated the diffusion coefficient for the two modes. The presence of two diffusion coefficients $D_{\text{internal}} \equiv \Gamma_{\text{internal}}/q^2|_{q\to 0}$ and $D_{\text{monomer}} \equiv \Gamma_{\text{monomer}}/q^2|_{q\to 0}$ is attributed to the coexistence of two different diffusive processes in the aggrecan samples, i.e., internal monomer dynamics and translational diffusion of aggrecan monomers (Figure 1). In the case of the aggregated sample, a few aggrecan monomers are free in solution, since the binding to the hyaluronan chain is physical and there is an equilibrated process of association. The amplitudes of the three dynamic processes (eq 3) are shown in the inset of Figure 3. All three modes are present in both self-assembled and monomeric aggrecan. Therefore in both the sample preparations, both the large and small species are present giving rise to three modes, "internal" for the fast internal dynamics of the aggrecan monomer, "monomer" for the translational diffusion of the monomers, and an "aggregate" mode whose relaxation time is outside the time window of the measured correlation function. The results for the monomer and the aggregate at different polymer concentrations are similar i.e., two diffusive modes are present and occur at similar relaxation rates.

The extrapolated diffusion coefficients D_{internal} and D_{monomer} are shown as a function of polymer concentration in Figure 4.

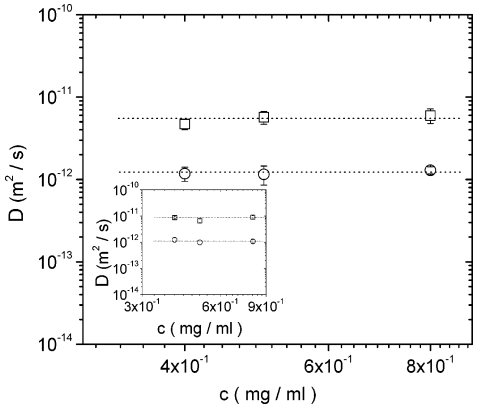

Figure 4. Diffusion coefficient as a function of polymer concentration for the monomeric aggrecan sample and for the aggregated aggrecan sample (inset). The dotted horizontal lines represent the average diffusion coefficient of each mode. The circles represent the mode due to the aggrecan monomer translational diffusion and squares the internal dynamics of the monomers.

Table 1. Hydrodynamics Radii of the Internal and Monomer Modes in the Monomeric and Aggregated Aggrecan Samples

	monomeric sample	aggregated sample
R_{internal} (nm)	44 ± 3	30 ± 3
R_{monomer} (nm)	202 ± 7	220 ± 10

There is no detectable dependence of the diffusion coefficients on the polymer concentration. This proves that the experiments were performed in the dilute solution regime. Indeed ~2 mg/mL has been reported as the overlap concentration for both the aggregated and the monomeric material[35] and the DLS experiments were performed at lower concentrations (<1 mg/mL). Table 1 shows the hydrodynamic radii of the monomer (R_h^{monomer}) calculated from the diffusion coefficient (D_{monomer}) by using the Stokes−Einstein relation

$$R_h^{\text{monomer}} = \frac{k_B T}{6\pi\eta_s D_{\text{monomer}}} \tag{6}$$

for the monomer and similarly the internal dynamic modes of the monomer (R_h^{internal}) can be calculated from the fast diffusion coefficient (D_{internal}). The hydrodynamic radii R_h^{monomer} and R_h^{internal} were found to be 202 ± 10 and 44 ± 7 nm respectively for the monomeric sample.

Small Angle Neutron Scattering. For small angle neutron scattering (SANS) experiments, aggregated material was dissolved in 0.15 M deuterated NaCl pH 7 buffer. A range of aggrecan concentrations were studied and the scattering cross section ($I(q)$) as a function of scattering wave vector (q) was obtained (Figure 5). The appearance of a small but well-defined correlation peak ($q = q^*$) allowed the correlation length ($\xi = 2\pi/q^*$) to be plotted as a function of polymer concentration (c, Figure 5 inset). The scaling law found for aggrecan aggregate $\xi \propto c^{-0.47\pm0.04}$ is consistent with the exponent (0.5) expected for linear flexible polyelectrolytes[27] and observed previously with flexible polyelectrolyte (polystyrene sulfonate) combs[1] in semidilute solutions. No evidence was found for liquid crystalline phases of the whole aggrecan aggregates. In contrast to previous experiments with glycoprotein samples all the scattering patterns were isotropic.[3]

Microrheology. *Particle Tracking.* Video particle tracking experiments were performed on monomeric and aggregated aggrecan in pH 7.4 EDTA buffer with 0.15 M NaCl. Amino

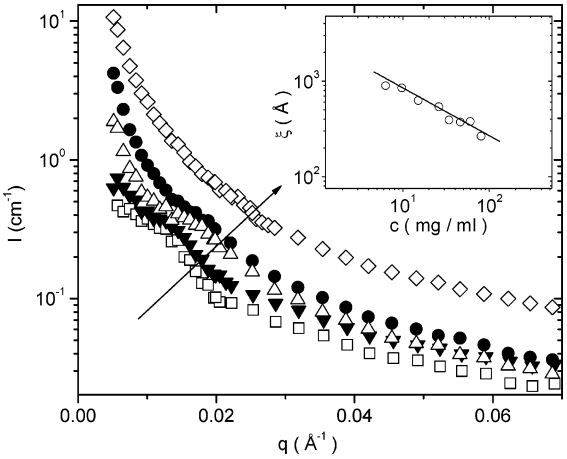

Figure 5. SANS scattering profiles for aggrecan aggregate as a function of polymer concentration in 0.15 NaCl pH 7 buffer in D_2O. The arrow indicates the shift of the correlation peak to higher q-values as the concentration increases. The concentration of aggrecan is 15 (squares), 26 (down triangles), 46 (up triangles), 60 (circles), and 80 mg/mL (diamonds). Inset: Correlation length as a function of polymer concentration for aggrecan aggregate. The straight line is the theoretical prediction of eq 7 (see discussion section).

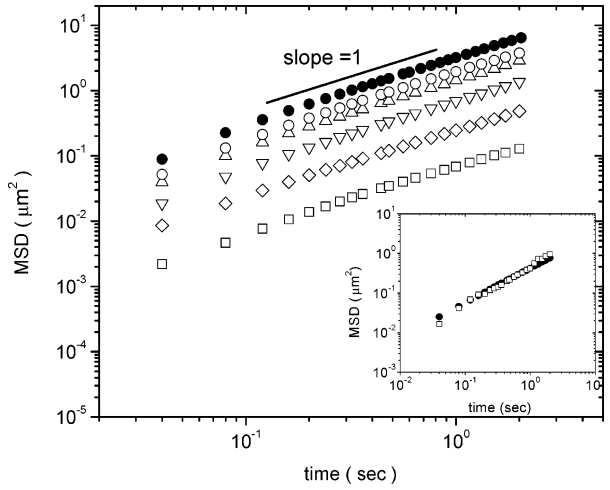

Figure 6. Particle tracking MSDs of 0.495 μm amino particles as a function of time for aggrecan monomer in pH 7.4 with 0.15 M NaCl. Several polymer concentrations are shown, 0.2 (open circles), 1 (up triangles), 3 (down triangles), 6 (diamonds), and 12 mg/mL (squares), including the case of pure solvent (closed circles). Not all of the measured MSDs are shown for clarity. A line with slope 1 indicates the diffusive behavior of the spheres in the solutions. Inset: One-point (closed symbols) and two-point (open symbols) particle tracking MSDs in monomeric 5 mg/mL aggrecan solution.

functionalized polystyrene particles of 0.495 μm diameter were used. Mean squared displacements (MSD) as a function of time for different polymer concentrations are shown in Figure 6. The reliability of the one-point microrheology data was tested using two-point microrheology. The resulting MSDs from one- and two-point microrheology are shown in Figure 6 inset for the monomeric material. The good agreement between one- and two-point correlation in both monomeric and aggregated samples proves that the bulk properties of the solutions were measured in particle tracking experiments.[39]

The MSDs from aggrecan solutions were predominantly viscous, as shown from the slope of the curves of Figure 6 for the case of the aggrecan monomer. Therefore, the diffusion coefficient of the probe spheres can be extracted ($MSD = 4Dt$) and subsequently the viscosity from the Stoke's Einstein equation ($\eta = k_BT/6\pi Da$, where a is the radius of the probe

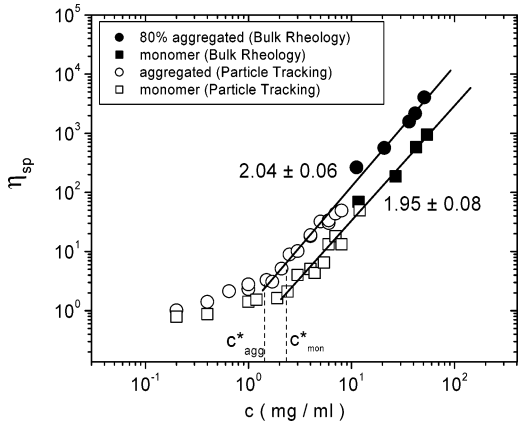

Figure 7. Specific viscosity of aggrecan monomer and aggregate in pH 7.4 with 0.15 M NaCl, as a function of polymer concentration as measured by particle tracking microrheology. Comparison of particle tracking data with previous bulk rheology data.[19] Power-law fits to the data for concentrations above the overlap concentration ($c > c^*$) and the corresponding scaling exponents are shown. Values of the overlap concentration are shown for the aggregate (c^*_{agg}) and the monomer (c^*_{mon}).

sphere). The specific viscosity ($\eta_{sp} = (\eta_{solution} - \eta_{solvent})/\eta_{solvent}$) of the aggrecan solutions as a function of aggrecan concentration is shown in Figure 7. Good agreement of the micorheology results is also shown with the viscosity/concentration scaling at higher polymer concentrations with bulk rheology.[19]

The power law dependence of the viscosity for aggrecan monomer and aggregate is similar to that found for densely grafted synthetic polyelectrolyte combs.[2] This dependence on polymer concentration can be attributed to the dense grafting of charged chains (GAGs) onto the aggrecan monomers inducing entangled reptative dynamics of the polymer backbone (Appendix).

Diffusing Wave Spectroscopy. The DWS experiments were performed in the transmission geometry with amino functionalized polystyrene spheres of 0.495 μm diameter, identical to those used for VPT. The mean free path (eq 2) for the spheres in water was $l^* = 420$ μm. The aggrecan samples were studied under identical conditions to the particle tracking experiments and over the same polymer concentration range. The correlation functions shifted to longer times as the polymer content increased (Figure 8 inset). The MSDs corresponding to the correlation functions are shown in Figure 8. The aggrecan solutions showed viscoelastic behavior at the high frequencies probed with DWS. Viscoelastic shear moduli of aggrecan monomer solutions are shown in Figure 9. The contribution of the solvent ($\eta_{solvent}\omega$) to the loss modulus (G'') was subtracted from the data, so that comparison to theoretical models for polymer dynamics could be made. The viscoelasticity of aggrecan solutions at high frequencies (probed by DWS) obeyed the predictions for Rouse dynamics, as found for the synthetic polyelectrolyte combs.[2] The shear moduli (G', G'') scaled as $\omega^{1/2}$ and the elastic modulus was approximately equal to the loss modulus ($G' \approx G''$).

Discussion

Solution Structure. Dynamic light scattering (DLS) on dilute aggrecan solutions allowed the measurement of the hydrodynamic radii of the internal modes of a monomer (44 ± 7 nm) and the size of a monomer (202 ± 10 nm). The monomer size is in reasonable agreement with AFM[26] and electric birefringence experiments.[32] The fast mode corresponds to internal

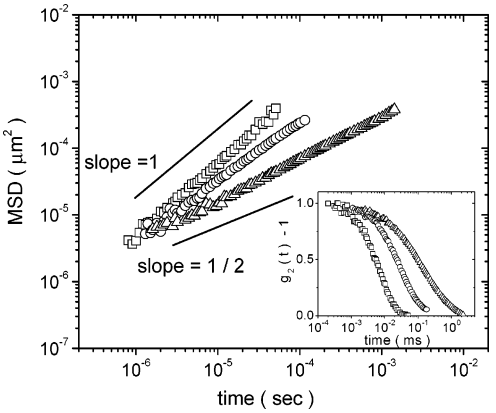

Figure 8. MSDs of 0.495 μm amino functionalized polystyrene spheres in buffer (squares) and in solutions of aggrecan monomer 2 (circles) and 12 mg/mL (triangles). Diffusive (1) and subdiffusive (1/2) scaling laws are shown to highlight the viscoelastic nature of the aggrecan solutions as probed by DWS. Inset: Intensity autocorrelation functions (from DWS in transmission geometry) from 0.495 μm amino functionalized polystyrene spheres in buffer (squares) and in solutions of aggrecan monomer with concentrations of 2 (circles) and 12 mg/mL (triangles).

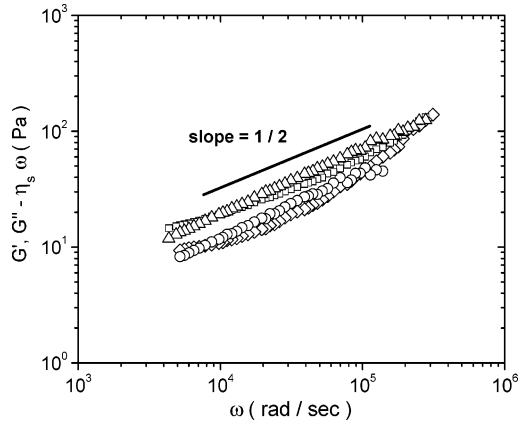

Figure 9. Viscoelastic moduli of 4 mg/mL aggrecan monomer (G' with diamonds and G'' with circles) and 10 mg/mL aggregate (G' with squares and G'' with triangles) in pH 7.4 buffered solution with 0.15 M NaCl. A line with slope 1/2 indicates the power law behavior.

longitudinal breathing modes of the aggrecan monomer side-chains. In analogy with the dynamics of planar polymer brushes,[55] semidilute solutions[42] and gels,[43] we identify the size of the internal mode with the internal hydrodynamic mesh size of an aggrecan monomer. The measured monomer mesh size (37 nm) is an order of magnitude larger than the size between GAG side-chains found with AFM,[33] ~3 nm, but close in to the side-chains of the cylindrical monomer brushes (~40 nm). This could either imply a transverse modulation of the side-chain structure of the monomers, e.g., a helical modulation of the density of the polyelectrolyte side-chains[44] increasing the hydrodynamic mesh of the side-chains, or longitudinal relaxation of the polymer brushes similar to the planar scenario.[55]

Small-angle neutron scattering (SANS) was performed above a polymer concentration of 6 mg/mL on the aggregated aggrecan material. The overlap concentration of both the aggregated and monomeric material has been measured as ~2 mg/mL in previous fluorescence recovery after photobleaching experiments,[35] so we deduce the studies are in the semidilute regime. The SANS profiles from semidilute solutions of aggrecan aggregate showed a correlation peak (Figure 5) whose position (q^*) scaled with polymer concentration with an exponent (-0.47 ± 0.04) consistent with previous results from linear polyelectrolytes and polyelectrolyte combs.[1,45] The correlation length of aggrecan solutions ($\xi \approx 2\pi/q^*$) was calculated from the data as shown in the inset of Figure 5. This mesh size reaches a value of 100 nm at 6 mg/mL. We need to understand the origin of the mesh. For flexible polyelectrolytes (linear and comb), the correlation length is given by eq 7[27] where we have rescaled the concentration dependence using x to model the dominant contribution of aggrecan monomers to the molecular weight of the aggregate

$$\xi \approx \left(\frac{B_{HA}}{x b_{HA}}\right)^{1/2}\left(\frac{c(\mathrm{mg/mL})N_A}{\mathrm{MW}_{\mathrm{AggrecanMonomer}}}\right)^{-1/2} \quad (7)$$

where c is the concentration of aggrecan monomers in mg/mL, x is the number of hyaluronic acid monomers between two aggrecan monomers, B_{HA} is the degree of extension of the backbone, b_{HA} is the size of the hyaluronic acid monomer (for a linear flexible polyelectrolyte $B = Nb/L$, N is the number of monomers, b is the monomer repeat distance, and L is the end to end distance), and $\mathrm{MW}_{\mathrm{AggrecanMonomer}}$ is the molecular weight of the aggrecan monomers. We deduce that the whole overlapping aggrecan aggregates produce the measured correlation length. The distance between two bound aggrecan monomers along the hyaluronan chain reported previously at high degree of aggregation is known to be ~20 nm.[33] The sections of the hyaluronan chain are assumed to be fully stretched by the repulsion between the grafted aggrecan monomers.[26] The mass of the aggrecan aggregate is predominantly (99%) due to the aggrecan monomers. Therefore, the effective monomer mass of the backbone hyaluronan chain is equal to the mass of the aggrecan monomer. The molecular weight of the aggrecan monomer has been found[35] to be ~2.6 MDa, and eq 7 is used to calculate the correlation length (ξ) (Figure 5 inset). There is good agreement between experimental and theoretical data. A value of 60 nm was found for the distance (xb_{HA}/B_{HA}) between aggrecan monomers along the backbone hyaluronan chain, and therefore, the aggrecan aggregate we study is slightly less densely grafted than that reported previously.[35]

Dynamic Picture. At time scales probed by particle tracking, the aggrecan samples were predominantly viscous. The scaling of the viscosity as a function of polymer concentration (Figure 7), above the overlap concentration (~2 mg/ml), was similar to that found for densely grafted synthetic polyelectrolyte combs.[2] The viscosity of the aggregated material was higher than the viscosity of the monomers at all concentrations. This is because the attachment of the aggrecan monomers on the hyaluronan chain gives rise to a super-comb structure whose motion is much slower than that of the free monomers (Figure 1). Previous bulk rheology data[19] for the zero shear viscosity of aggrecan solutions is plotted on the same log−log plot as the particle tracking data (Figure 7).

The bulk rheology data of Figure 7 includes both lowly aggregated material (<5%) and highly aggregated material (80%). These were the extremes in aggregation content of the sample preparations measured in previous bulk rheology experiments.[19] For the preparations studied in this work, the aggrecan monomer sample is expected to contain predominantly aggrecan monomers, and the aggrecan aggregate sample is expected to contain predominantly aggrecan aggregate. The drop in viscosity as a function of the degree of aggregation is observed by both microrheology and bulk techniques. Power-laws were able to fit both the data sets simultaneously (particle tracking and bulk rheology); $\eta \sim c^{\alpha}$ where η is the viscosity and α the exponent. An exponent of 2.04 ± 0.06 was found for the samples with

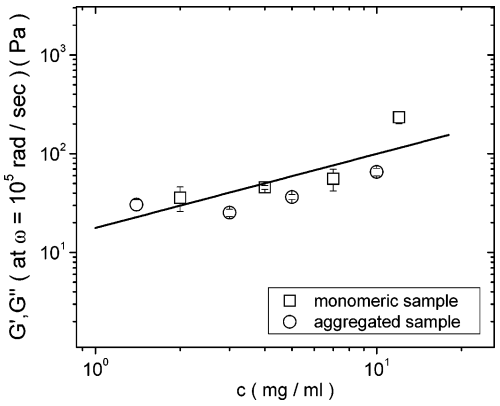

Figure 10. Viscoelastic moduli at $\omega = 10^5$ rad/s. The straight line is the theoretical prediction of eq 8.

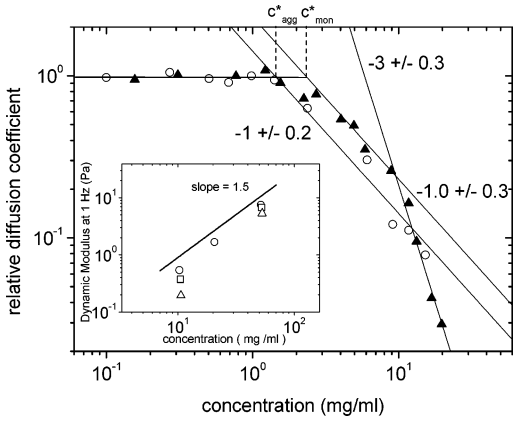

Figure 11. Self-diffusion coefficients for FRAP data[54] and (inset) the modulus (G) calculated from bulk rheology data at 1 Hz[19]. Values of the overlap concentration (c^*) are shown for the aggregate (c^*_{agg}) and the monomer (c^*_{mon}).

high aggregate content and an exponent of 1.95 ± 0.08 for the samples with low aggregate content. Even though the two techniques are not over the same polymer concentration range, the power-law fits show that there is good agreement between the measurements. Such high exponents for the scaling of the specific viscosity with polymer concentration have been previously seen with densely branched polystyrene sulfonate combs,[2] e.g., $\eta \sim c^2$ for densely branched PSS combs. A challenge for understanding the comb dynamics is the extremely low entanglement concentration in such materials (i.e., low concentration for the onset of reptation) and the absence of a semidilute unentangled regime above the overlap concentration.[2,28] The comb nature of aggrecan is seen to be vitally important to the low-frequency viscosity of the molecules. Artificial biomimetic boundary lubricants would need to be synthesized with flexible side-chain architectures to achieve equivalent rheological properties to aggrecan. Linear polyelectrolytes[46] do not offer an efficient mechanism for energy dissipation in soft solids due to the weak dependence of the viscosity on the polymer concentration $\eta \sim c^{1/2}_{\text{linear}}$ compared with the strong dependence of densely branched comb architectures (e.g., $\eta \sim c^2_{\text{comb}}$).

In the appendix, a possible explanation for the concentration dependence of the viscosity, modulus, and diffusion coefficient of aggrecan is presented. A dynamic scaling theory for the reptation of comb polyelectrolytes on polymer concentration (c) is described that simultaneously explains the viscosity of synthetic polyelectrolyte combs with high degrees of branching (Figure 12), the modulus (G) of aggrecan from previous bulk experiments ($G \sim c^{1.5}$, Figure 11), the diffusion coefficient of aggrecan from FRAP (Figure 11), and the viscosity (η) from

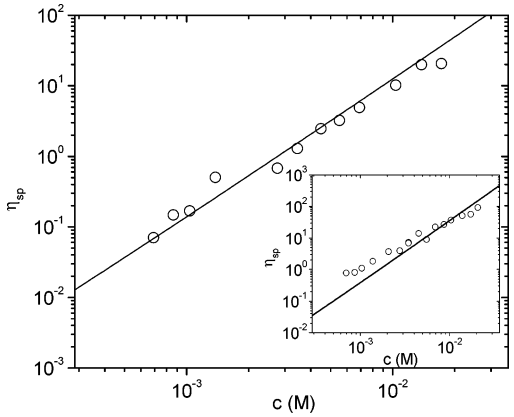

Figure 12. Fit of the model for comb reptation with unentangled side-chains for PSS (equation A8) with (a) large number of short side-chains and (b) small number of long side-chains.

the current microrheology results ($\eta \sim c^2$, Figure 7). Crucially the $c^{0.5}$ difference in the concentration dependence of the modulus and viscosity observed experimentally (we expect the standard relationship $\eta \approx G\tau$ to hold, where τ is the slowest relaxation time of the material) is attributed to the relaxation dynamics of the side-chains of the aggrecan monomers and this concentration dependence agrees with measurements of self-diffusion experiments in FRAP experiments ($D \sim R^2/\tau$, implying $D \sim c^{-1}$, eq A11, Figure 11, D is the diffusion coefficient, R is the chain backbone radius, and τ is the relaxation time). Furthermore, the dynamic scaling theory captures the results from previous bulk rheology experiments that the viscosity is proportional to the degree of aggregation. There is no exponential dependence of the viscosity on the polymer concentration (Figure 7), so we can rule out a model of reptation with entangled side-chains for aggrecan (equation A26) at the concentrations we measure and conclude the chains move by reptation with unentangled side-chains (eq A8).

At the high frequencies probed by diffusing wave spectroscopy (DWS), the aggrecan solutions were viscoelastic and showed the $\omega^{1/2}$ scaling of the shear modulus with frequency (ω) characteristic of the Rouse model (Figure 9). The analysis demonstrated previously for synthetic polyelectrolyte combs can be applied for the aggrecan solutions. The value of the moduli at a certain frequency is given by[2,27]

$$G'(\omega) \approx G''(\omega) \approx (\eta_s k_B T)^{1/2} \left(\frac{B_{BB}}{y b_{BB}}\right)^{-3/4} \left(\frac{c(\text{mg/mL}) N_A}{\text{MW}_{GAG}}\right)^{3/4} \omega^{1/2} \quad (8)$$

One aggrecan monomer consists of GAG chains grafted on a protein backbone (BB). A GAG chain has a molecular weight of 20 KDa (GAGs are the dominant contribution to the molecular weight of the aggrecan monomer), and the distance between GAG chains along the backbone is $y b_{BB}/B_{BB} = 3$ nm.[35] At high frequencies, we conclude that the internal dynamics of the aggrecan monomers are probed in both the aggregated and the monomeric samples, similar to polystyrene sulfonate combs.[2] Figure 10 shows the value of the viscoelastic moduli at $\omega = 10^5$ rad/s for the aggregated and the monomeric samples as a function of polymer concentration. There is no significant difference between the aggregated and the monomeric sample. Thus, the rheological properties are dominated by the internal dynamics of the aggrecan monomers at high frequencies (DWS) in both the aggregated and the monomeric material. The data are in good agreement with the prediction of eq 8 for the viscoelastic modes (Figure 10, continuous line). An estimation

of the values for the viscoelastic moduli assuming that the Rouse modes of the whole aggregate are observed predicts significantly lower values for the relaxation rates than those experimentally observed, again indicating that the origin of the viscoelasticity is interchain dynamic modes. A similar picture was developed with synthetic comb polyelectrolytes.[2]

Future work on proteoglycans will focus on the continued development of the dynamic scaling theory to explain the entangled dynamics of the comb molecules in solution. Furthermore additional structural information should be available from aggrecan oriented in a magnetic field using small-angle neutron scattering.[3] It would also be interesting to examine the nonlinear microviscoelasticity of aggrecan molecules using magnetic tweezers,[30,47] since this would help model the action of aggrecan in synovial joints.

Conclusions

The hydrodynamic radii of the aggrecan monomer and an internal longitudinal breathing mode of the aggrecan monomer were measured using dynamic light scattering. Small-angle neutron scattering (SANS) experiments with the aggregated material in semidilute solutions probed the correlation length (ξ) between the whole aggregates and standard linear polyelectrolyte scaling on the polymer concentration (c) was observed, $\xi \sim c^{-0.47\pm0.04}$. Video particle tracking (VPT) microrheology at low frequencies revealed the difference between aggregated and monomeric aggrecan. The aggregated material demonstrated much higher viscosities than the monomeric material. The scaling law of the intrinsic viscosity (η) as a function of polymer concentration was similar to that found for densely grafted polystyrene sulfonate combs[2]; $\eta \sim c^{2.04\pm0.06}$ and $\eta \sim c^{1.95\pm0.08}$ for the assembled and monomeric samples, respectively. The viscosity measured using VPT was consistent with conventional rheological data and results from the two particle cross-correlation tracking method. The microrheology at high frequencies (DWS) was dominated by the internal Rouse modes of the aggrecan monomers in both the aggregated and the monomeric material and was in agreement with the scaling expected for flexible polyelectrolyte chains. A dynamic scaling model was developed to describe the low-frequency viscoelasticity and dynamics of reptating polyelectrolyte combs and was in reasonable agreement with experiment. It is concluded that aggrecan reptates with unentangled dynamics of the side-chains of its monomers over the range of concentrations examined (0.2−50 mg/mL).

Appendix

We extend the analysis of polyelectrolyte comb rheology previously presented in unentangled semidilute solutions of polystyrene sulfonate combs to the concentrated reptating regime.[2] Aggrecan monomers are modeled as homopolyelectrolytes (with the same expansion coefficients (B) for the backbones and side-chains) to simplify the analysis and to indicate the general features involved in the dynamics. We use the simplest method of defining the entanglement concentration (c_e). We assume that there are a fixed number of chains (n) at the entanglement concentration that are required to provide the topological constraints for reptation. Following Dobrynin et al.,[27,28] a is defined to be the size of the tube for reptation. We assume, as for a linear polyelectrolyte, that the size of the tube is proportional to the number of overlapping chains at the entanglement concentration (n) multiplied by the correlation length (ξ)

$$a \approx n\xi \tag{A1}$$

As in the case of linear flexible polyelectrolytes, the entanglement strand is the length of backbone in the sphere of radius a and is a random walk of backbone blobs (there are N_e monomers in an entanglement strand)

$$\frac{N_e}{g} \approx \left(\frac{a}{\xi}\right)^2 \tag{A2}$$

By definition when the comb polyelectrolyte chains start reptating there are n strands in the volume a^3. Combining (A1) and (A2) gives an expression for n in terms of the length of an entanglement strand (N_e) and the number of monomers in a blob (g)

$$\frac{N_e}{g} = n^2 \tag{A3}$$

This is an identical expression to that found with linear flexible polyelectrolytes.

(a) Reptation with Unentangled Side-Chains. Following our previous results for unentangled polyelectrolyte combs,[2] the expression for the reptation time of comb polyelectrolytes contains one additional term compared with the linear result. The additional term ($1 + sm^2/Kg$, s is the number of attached side chains, m is the number of monomers on a side chain, g is the number of monomers in a blob, and K is the number of monomers along the backbone) renormalizes the backbone blob time to account for the dynamics of the attached side chains. This renormalization is not trivial, since it introduces an additional concentration dependence in the relaxation time (through g) and captures the cross over between Zimm and Rouse dynamics at the static mesh size of the combs. Following the reasoning for linear polyelectrolyte reptation,[27,28] the comb reptation time for a polyelectrolyte comb is

$$\tau_{rep} \approx \frac{\eta_s b^3}{kT}\left(1 + \frac{sm^2}{Kg}\right) n^{-2} K^3 B^{-3} \tag{A4}$$

where η_s is the solvent viscosity, b is the monomer size, kT is the thermal energy, and B is the expansion coefficient of the chain.

The expression for the modulus (G) is unchanged from the linear flexible polyelectrolyte result

$$G \approx \frac{kT}{a^2\xi} \tag{A5}$$

where ξ is the static correlation length.

Therefore, substituting in the expressions for a and ξ (eq A1 and $\xi = (B/cb)^{1/2}$), we have an expression for the modulus as a function of the polymer concentration (c)

$$G \approx \frac{kT}{n^2}\left(\frac{cb}{B}\right)^{3/2} \tag{A6}$$

The $c^{3/2}$ dependence of the modulus from this flexible polyelectrolyte scaling theory is clearly followed in the experimental data of the inset of Figure 11 from bulk rheology experiments on aggrecan.[19]

The prediction for semiflexible polymer scaling is $G \sim c^{1.4}$, underestimating the concentration dependence of aggrecan and

no additional concentration of the viscosity is predicted ($\eta \sim c^{1.4}$),[48] since the conformation of the chains do not depend strongly on the polymer concentration. A completely semiflexible model for the backbone and side chains can thus be ruled out for aggrecan.

The slight variation in modulus with degree of aggregation (inset, Figure 11) is thought to be related to changes in the size of the tube (or equivalently the number of overlapping chains required for reptation, n in eq A6). The final expression for the viscosity is approximated in the standard way by the modulus multiplied by the slowest relaxation time in the system

$$\eta \approx G\tau \tag{A7}$$

which is therefore

$$\eta \approx \eta_s K^3 (cb^3)^{3/2} B^{-9/2} \left(1 + \frac{sm^2}{K}\left(\frac{b}{B}\right)^{3/2} c^{1/2}\right) n^{-4} \tag{A8}$$

where we have used the result $g = c\xi^3$. Fits are shown of the model to highly branched synthetic polystyrene comb polyelectrolytes (Figure 12).[2] The model gives reasonable values for both the number of chains for reptative motion ($\sim$4) and the degree of extension of the chains (B) which is 2−3 in agreement with X-ray/SANS results.[1] No other fit parameters are required to describe the experimental data. The fits are slightly better on Figure 12 for the short side-chain PSS comb polyelectrolytes, which could be due to the introduction of reptative modes in the long comb side-chain samples (inset, Figure 12). Similarly, reasonable agreement was found with glycoprotein solutions.[49] These samples have short side chains, no signature of the concentration dependence of the side-chain dynamics is observed, and a $\eta \sim c^{3/2}$ viscosity dependence was measured above the overlap concentration.

The model described by equation (A8) predicts the concentration dependence observed for aggrecan aggregate and aggrecan monomer ($\eta \sim c^2$ and $c^{1.9}$ respectively). The hyaluronic acid backbone does not provide a large additional concentration dependence on the relaxation time of an aggregate, since it is fairly rigid in the aggregated state and corresponds to a semiflexible polymer[26] (there is therefore little concentration dependence of the hyaluronan length and thus its relaxation time is also concentration independent[48]).

The diffusion coefficient (D_{self}) for the polyelectrolyte combs can also be calculated from such a scaling analysis

$$D_{self} \approx \frac{R^2}{\tau} \tag{A9}$$

where R is the size of the comb backbone and for a flexible polyelectrolyte in semidilute solutions it is given by

$$R \approx \left(\frac{K}{c\xi}\right)^{1/2} \tag{A10}$$

Therefore, substituting in expressions for R (A10) and the reptation time (τ, A4)

$$D_{self} \approx \left(\frac{kT}{\eta_s b^{5/2}}\right) n^2 K^{-2} c^{-1/2} B^{5/2} \left(1 + \frac{sm^2}{K}\left(\frac{b}{B}\right)^{3/2} c^{1/2}\right)^{-1} \tag{A11}$$

The c^{-1} dependence of the diffusion coefficient is in agreement with FRAP data for aggrecan (Figure 11) for the majority of concentrations measured. The power law fits are preferable to the stretched exponential model of Philies,[50] since they provide the more physical result that the overlap concentration (c^*) is lower for aggrecan aggregates than monomers. There is reasonable agreement in the values of c^* calculated using FRAP and particle tracking (Figures 7 and 11). Furthermore in the current model these values of c^* are identified with the concentration at which the combs start reptating (c_e) and thus $c^* \approx c_e$.

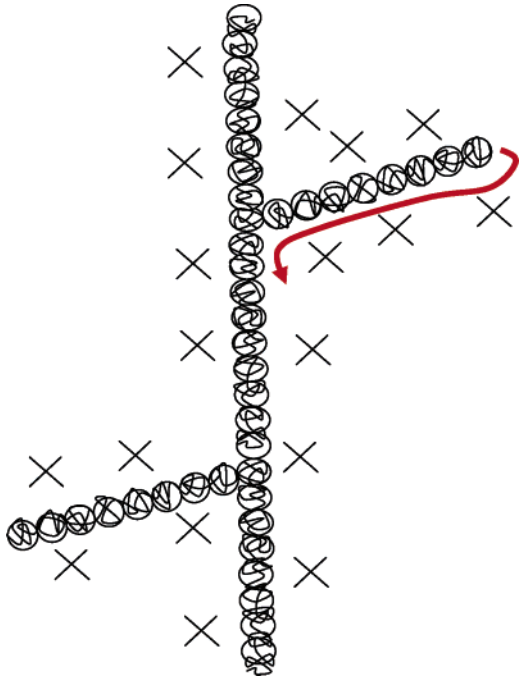

Figure 13. Schematic diagram showing the process of activated reptation of side-chain motion with flexible comb polyelectrolytes. The charged blob conformation of the aggrecan monomer side-chain and backbone is highlighted.

(b) Entangled Side-Chain Comb Reptation. When the side chains of a polyelectrolyte comb are sufficiently long or the concentration sufficiently high, the side chains can become entangled and the calculation of the viscoelasticity is a more complex problem. With melt polymer dynamics the influence of the side-chain motion is solved through the solution of a Kramers type problem (the transition over a potential barrier), and this is the approach we will follow.[14]

From Doi and Edwards,[52] the potential ($U(\Delta L)$) for the Kramer's problem for the retraction of a Gaussian chain by a distance (ΔL) is given by

$$U(\Delta L) = \alpha kT \frac{(\Delta L^2)}{R^2} \tag{A12}$$

where α is a number of order unity and kT is the thermal energy. The Gaussian approximation for the conformational statistics of a polymer chain is reasonable with flexible polyelectrolytes in the semidilute regime above the overlap concentration, since the charge interaction is screened beyond the static mesh size of the polyelectrolyte chains.[27] The spring constant for entropic force opposing compression of the guassian polyelectrolyte is proportional to R^{-2} where R is the undeformed radius of gyration given by (A10, where K is replaced by m in this case).[53] For a side-chain composed of charged blobs in a side tube the length of complete arm retraction (Figure 13) is

$$\Delta L = \left(\frac{m}{N_e}\right) a \tag{A13}$$

where a is the tube diameter, m is the number of monomers in

a side-chain, and N_e is the entanglement length. Therefore, from the solution of the Kramer's problem,[52] the time for a flexible polyelectrolyte arm to retract is

$$\tau_1 \sim \frac{(\Delta L)^2}{D_{||}} \exp\{U(\Delta L)/kT\} = \frac{(\Delta L)^2}{D_i} \exp\left\{\alpha m n^{-2} c^{1/2} \left(\frac{b}{B}\right)^{3/2}\right\} \quad \text{(A14)}$$

where $D_{||}$ is the diffusion coefficient for the motion of the arm parallel to the tube.

Substituting in the expression for ΔL (eq A13), we have

$$\tau_1 \sim \left(\frac{m}{N_e}\right)^2 \frac{a^2}{D_{||}} \exp\left\{\alpha m n^{-2} c^{1/2} \left(\frac{b}{B}\right)^{3/2}\right\} \quad \text{(A15)}$$

For the curvilinear diffusion coefficient $D_{||}$, we will use the expression from Dobrynin et al.[27] for entangled linear flexible polyelectrolytes. It is

$$D_{||} = \left(\frac{kT}{\eta_s}\right) n^2 m^{-2} b^{5/2} c^{-1/2} B^{5/2} \quad \text{(A16)}$$

Therefore from equation (A15) the arm retraction time is given by

$$\tau_1 \sim N_e^{-2} a^2 \left(\frac{\eta_s b^{5/2}}{kT}\right) n^{-2} m^4 c^{1/2} B^{-5/2} \exp\left\{\alpha m n^{-2} c^{1/2} \left(\frac{b}{B}\right)^{3/2}\right\} \quad \text{(A17)}$$

We then use the expression for the tube diameter (a), and combining (A1) and (A3) we have

$$a^2 = \frac{N_e}{g} \xi^2 \quad \text{(A18)}$$

Substituting in eq A17 gives

$$\tau_1 \sim N_e^{-1} \left(\frac{\xi^2}{g}\right) \left(\frac{\eta_s b^{5/2}}{kT}\right) n^{-2} m^4 c^{1/2} B^{-5/2} \exp\left\{\alpha m n^{-2} c^{1/2} \left(\frac{b}{B}\right)^{3/2}\right\} \quad \text{(A19)}$$

For comb polyelectrolytes we know the entanglement length N_e (eq A3) and therefore

$$\tau_1 \sim m^4 \frac{\xi^2}{g^2 n^4} \left(\frac{\eta, b^{5/2}}{kT}\right) c^{1/2} B^{-5/2} \exp\left\{\alpha m n^{-2} c^{1/2} \left(\frac{b}{B}\right)^{3/2}\right\} \quad \text{(A20)}$$

From Dobrynin et al.[27] and our static picture of comb polyelectrolytes,[1] we have expressions for the correlation length (ξ) and the number of monomers in a blob (g)

$$\xi = \left(\frac{B}{cb}\right)^{1/2} \quad \text{(A21)}$$

$$g = \left(\frac{B}{b}\right)^{3/2} c^{-1/2} \quad \text{(A22)}$$

Therefore, the relaxation time for the side-chains of a comb is

$$\tau_1 \sim m^4 c^{1/2} B^{-9/2} b^{9/2} n^{-4} \left(\frac{\eta_s}{kT}\right) \exp\left\{\alpha m n^{-2} c^{1/2} \left(\frac{b}{B}\right)^{3/2}\right\} \quad \text{(A23)}$$

For a complete comb with entangled side-chains the reptation time[53] of the backbone is given by

$$\tau_{rep} = \tau_1 (s-2) \left(\frac{K}{N_e}\right)^2 \quad \text{(A24)}$$

where s is the number of side-chains and the friction is dominated by the slow activation dynamics of the side-chains. Substituting (A22) and (A3) into (A24), we have

$$\tau_{rep} = \tau_1 (s-2) K^2 n^{-4} \left(\frac{b}{B}\right)^3 c \quad \text{(A25)}$$

As before, the modulus is given by (A6) in agreement with the experiment. The viscosity for a comb with entangled side-chains is calculated from (A7)

$$\eta = c^3 n^{-10} (s-2) m^4 K^2 \left(\frac{b}{B}\right)^9 \eta_s \exp\left\{\alpha m n^{-2} c^{1/2} \left(\frac{b}{B}\right)^{3/2}\right\} \quad \text{(A26)}$$

This high concentration dependence of the viscosity is not observed in either the PSS comb polyelectrolytes (Figure 12) or the aggrecan samples (Figure 7). This would appear to rule out the possibility of entangled side-chain reptation dynamics in these polyelectrolyte systems.

Furthermore the self-diffusion coefficient for reptation with entangled side-chains can be calculated from (A9) giving

$$D_{self} \sim c^{-2} \exp\left\{-\alpha m n^{-2} c^{1/2} \left(\frac{b}{B}\right)^{3/2}\right\} n^8 K^{-1} m^{-4} \times \left(\frac{kT}{\eta_s (s-2)}\right) B^7 b^{-7} \quad \text{(A27)}$$

Such a behavior ($D_{self} \sim c^{-2}$ or a stronger polymer concentration dependence) is not in agreement with the FRAP data from either aggrecan aggregate or monomer at low concentrations (Figure 11[35]). However, it could explain the sharp increase in diffusion times with the aggrecan monomers at high concentrations (>20 mg/mL).

Acknowledgment. We thank Edoardo de Luca for helping set up the microrheology experiments and the EPSRC for funding T.A.W. and A.P. Dr. Ralph Colby, Amalia Aggeli, Gleb Yakubov, Christine Fernyhough, and Tanniemola Liverpool are thanked for useful conversations.

References and Notes

(1) Papagiannopoulos, A.; Fernyhough, C. M.; Waigh, T. A.; Radulescu, A. *Polymer* **2005**, submitted.
(2) Papagiannopoulos, A.; Fernyhough, C. M.; Waigh, T. A. *J. Chem. Phys.* **2005**, *123*, 214904.
(3) Waigh, T. A.; Papagiannopoulos, A.; Voice, A.; Bansil, R.; Unwin, A. P.; Dewhurst, C.; Turner, B.; Afdhal, N. *Langmuir* **2002**, *18*, 7188−7195.
(4) Bansil, R.; Stanley, E.; LaMont, J. T. *Annu. Rev. Physiol.* **1995**, *57*, 635−657.
(5) Cao, X.; Bansil, R.; Bhaskar, K. R.; Turner, B. S.; LaMont, J. T.; Niu, N.; Afdhal, N. H. *Biophys. J.* **1999**, *76*, 1250−1258.
(6) Bhaskar, K. R.; Garik, P.; Turner, B. S.; Bradley, J. D.; Bansil, R.; Stanley, H. E.; LaMont, J. T. *Nature* **1992**, *360*, 458−461.
(7) http://www.glycoforum.gr.jp.
(8) Iozzo, R. V. *Proteoglycans: structure, biology and molecular interaction*; Marcel Dekker: New York, 2000.
(9) Ruhe, J.; Ballauff, M.; Biesalski, M.; Dziezok, P.; Grohn, F.; Johannsmann, D.; Houbenov, N.; Hugenberg, N.; Konradi, R.; Minko, S.; Motornov, M.; Netz, R. R.; Schmidt, M.; Seidel, C.; Stamm, M.; Stephan, T.; Usov, D.; Zhang, H. N. *Adv. Polym. Sci.* **2004**, *165*, 79−150.
(10) Viney, C.; Huber, A. E.; Verdugo, P. *Macromolecules* **1993**, *26*, 852.
(11) Jin, M. S.; Grodzinsky, A. J. *Macromolecules* **2001**, *34*, 8330−8339.
(12) Puxkandl, R.; Zizak, I.; Paris, O.; Keckes, J.; Tesch, W.; Bernstorff, S.; Purslow, P.; Fratzl, P. *Philos. Trans. R. Soc. London B* **2002**, *357*, 191−197.

(13) Hull, D.; Clyne, T. W. *An Introduction to Composite Materials*; Cambridge University Press: New York, 2001.
(14) Daniels, D. R.; T. C. B. M.; Crosby, B. J.; Young, R. N.; Fernyhough, C. M. *Macromolecules* **2001**, *34*, 7025−7033.
(15) Colby, R. H.; Gillmor, J. R.; Galli, G.; Laus, M.; Ober, C. K.; Hall, E. *Liq. Cryst.* **1993**, *13*, 233−245.
(16) Kannan, R. M.; Kornfield, J. A.; Schwenk, N.; Boeffel, C. *Macromolecules* **1993**, *26*, 2050−2056.
(17) Soby, L.; Jamieson, A. M.; Blackwell, J.; Choi, H. U.; Rosenberg, L. C. *Biopolymers* **1990**, *29*, 1587−1592.
(18) Meechai, N.; Jamieson, A. M.; Blackwell, J.; Carrino, D. A.; Bansal, R. *Biomacromolecules* **2001**, *2*, 780−787.
(19) Hardingham, T. E.; Muir, H.; Kwan, M. K.; Lai, W. M.; Mow, V. C. *J. Orthop. Res.* **1987**, *5*, 36−46.
(20) B. M. Vertel, A. R. In *Proteoglycan: Structure, Biology and Molecular Interactions*; Iozzo, R. V., Ed.; Marcel Dekker: New York, 2000; pp 343−377.
(21) Gong, J. P.; Osada, Y. *Prog. Polym. Sci.* **2002**, *27*, 3−38.
(22) Cleland, R. L. *Arch. Biochem. Biophys.* **1977**, *180*, 57−68.
(23) Krause, W. E.; Bellomo, E. G.; Colby, R. H. *Biomacromolecules* **2001**, *2*, 65−69.
(24) Fouissac, E.; Milas, M.; Rinaudo, M. *Macromolecules* **1993**, *26*, 6945−6951.
(25) Rinaudo, M.; Milas, M.; Jouon, N.; Borsali, R. *Polymer* **1993**, *34*, 3710−3715.
(26) Dean, D.; Han, L.; Ortiz, C.; Grodzinsky, A. J. *Macromolecules* **2005**, *38*, 4047−4049.
(27) Dobrynin, A. V.; Colby, R. H.; Rubinstein, M. *Macromolecules* **1995**, *28*, 1859−1871.
(28) Dobrynin, A. V.; Rubinstein, M.; Colby, R. H. *Phys. Rev. Lett.* **1994**, *73*, 2776−2779.
(29) Perkins, S. J.; Nealis, A. S.; Dunham, D. G.; Hardingham, T. E.; Muir, H. I. *Biochem. J.* **1992**, *285*, 263−268.
(30) Waigh, T. A. *Rep. Prog. Phys.* **2005**, *68*, 685−742.
(31) Tseng, Y.; Wirtz, D. *Biophys. J.* **2001**, *81*, 1643−1656.
(32) Foweraker, A. R.; Isles, M.; Jennings, B. R.; Hardingham, T. E.; Muir, H. *Biopolymers* **1977**, *16*, 1367−1369.
(33) Ng, L.; Grodzinsky, A. J.; Patwari, P.; Sandy, J.; Plaas, A.; Ortiz, C. *J. Struct. Biol.* **2003**, *143*, 242−257.
(34) Hardingham, T. E. *Biochem. J.* **1979**, *177*, 237−247.
(35) Gribbon, P.; Hardingham, T. E. *Biophys. J.* **1998**, *75*, 1032−1039.
(36) MacKintosh, F. C.; Schmidt, C. F. *Curr. Opin. Colloid Interface Sci.* **1999**, *4*, 300−307.
(37) Mason, T. G.; Weitz, D. A. *Phys. Rev. Lett.* **1995**, *74*, 1250−1253.
(38) http://www.physics.emory.edu/∼weeks/idl/tracking.html.
(39) Crocker, J. C.; Valentine, M. T.; Weeks, E. R.; Gisler, T.; Kaplan, P. D.; Yodh, A. G.; Weitz, D. A. *Phys. Rev. Lett.* **2000**, *85*, 888−891.
(40) Xu, J.; Palmer, A.; Wirtz, D. *Macromolecules* **1998**, *31*, 6486-6492.
(41) Mason, T. G.; Ganesan, K.; van Zanten, J. H.; Wirtz, D.; Kuo, S. C. *Phys. Rev. Lett.* **1997**, *79*, 3282−3285.
(42) de Gennes, P. G. *Scaling Concepts in Polymer Physics*; Cornell University Press: Ithica, NY, 1979.
(43) Tanaka, T.; Hocker, L. O.; Benedek, G. B. *J. Chem. Phys.* **1973**, *59*, 5151−5159.
(44) Fazli, H.; Golestanian, R.; Kolahchi, M. R. *Phys. Rev. E* **2005**, *72*, 011805.
(45) de Gennes, P. G.; Pincus, P.; Velasco, R. M.; Brochard, F. J. *J. Phys. (Paris)* **1976**, *37*, 1461.
(46) Boris, D. C.; Colby, R. H. *Macromolecules* **1998**, *31*, 5746−5755.
(47) Uhde, J.; Feneberg, W.; Ter-Oganessian, N.; Sackmann, E.; Boulbitch, A. *Phys. Rev. Lett.* **2005**, *94*, 1981021−1981024.
(48) Morse, D. C. *Macromolecules* **1998**, *31*, 7044−7067.
(49) Yakubov, G. unpublished data, 2005.
(50) Phillies, G. D. J. *J. Phys. Chem.* **1989**, *93*, 5029−5039.
(51) See reference 14.
(52) Edwards, S. F.; Doi, M. *The Theory of Polymer Dynamics*; Oxford University Press: New York, 1986.
(53) Rubinstein, M.; Colby, R. H. *Polymer Physics*; Oxford University Press: New York, 2003.
(54) Gribbon, P.; Hardingham, T. E. *Biophys. J.* **1998**, *75*, 1032−1039.
(55) de Gennes, P. G. *C. R. Acad. Sc. Paris* **1986**, *302*, 765−768.

BM060287D